BAI-Net: Individualized Human Cerebral Cartography using Graph Convolutional Network

Liang Ma, Yu Zhang, Hantian Zhang, Luqi Cheng, Junjie Zhuo, Weiyang Shi, Yuheng Lu, Wen Li, Zhengyi Yang, Jiaojian Wang, Lingzhong Fan and Tianzi Jiang

***Abstract*—Individualized human cerebral cartography has drawn considerable attention in neuroscience research. But many challenges remain, mainly due to large cross-subject variations in brain morphology, connectivity, and function. We developed a new tool called brain atlas individualization network (BAI-Net) that automatically parcels individual cerebral cortex into segregated functional areas using structural and diffusion MRIs. The presented method integrates the group priors into the loss function of graph convolution network, and learns the connectivity context of anatomical fingerprints for each area on individual brain graphs. The presented model provides reliable, efficient and explainable individual cortical parcellations across multiple sessions with different scanners. Moreover, it keeps highly group consistence as well as individual-specific variations. Given the reliable inter-subject variabilities from BAI-Net's parcellation, their functional connectome showed higher associations with individual behavioral scores in a cognitive battery, compared to the individualized methods. The presented model has potential applications in locating more individual-specific regions in the diagnosis and treatment of neurological disorders, rather than group-registered method in terms of cortical morphology. And its methodology could be applied to individualize many population brain atlases.**

***Index Terms*— cerebral cartography, individual parcellations, functional alignment, anatomical fingerprints, graph convolutional network.**

I. INTRODUCTION

The human cerebral cortex can be divided into multiple function-specific areas in terms of distinct in vivo and ex vivo features. To understand the functional organization of the human brain, neuroanatomists have built a variety of brain atlases to depict cyto-, myelo-, receptor-, and anatomical brain architectures using a few postmortem human brains [1-7]. As the technology advances, magnetic resonance imaging (MRI) techniques, have been used to investigate in vivo brain features (e.g., macrostructure, connectivity, and functional activations) as well as to make subsequent cartographic explorations of the human cerebral cortex at the population level [8-16]. However, morphology registration might not be reflected individual cortical variations. Many studies presents the individual variations in areal size, location, spatial arrangement, and connectivity patterns, as a result of genetic and environmental influences, [15, 17]. It would improve cross-subject analysis and reveal behavior-related, disease-dependent locations for personalized medical practice with more precise functional references [18-24].

Many studies adopted cortical fingerprint-based (e.g., anatomical and functional connectivity) mappings for individualizing the population atlas to reveal individual-specific variability of cortical areas [13, 25-33]. Population atlas priors provide a blueprint of functional and anatomical architectures of the human brain in these mappings to guide individual-specific topography presented by connection fingerprints [13, 23, 26, 32-37]. However, there still exists a great challenge for achieving a robust, individual-specific

Manuscript received July 12, 2021. This work was partially supported by the Natural Science Foundation of China (Grant Nos. 91432302, 31620103905 and 81701781), the Science Frontier Program of the Chinese Academy of Sciences (Grant No. QYZDJ-SSW-SMC019), National Key R&D Program of China (Grant No. 2017YFA0105203), Beijing Municipal Science & Technology Commission (Grant Nos. Z161100000216152, Z161100000216139, Z171100000117002), Beijing Advanced Discipline Fund, the Guangdong Pearl River Talents Plan (2016ZT06S220), Major Scientific Project of Zhejiang Lab (No. 2020ND8AD01), Youth Innovation Promotion Association Chinese Academy System (CAS). (Corresponding auther: Tianzi Jiang and Lingzhong Fan).

Liang Ma, Hantian Zhang, Weiyang Shi, Yuheng Lu, Wen Li, Zhengyi Yang and Lingzhong Fan are with the School of Artificial Intelligence, University of Chinese Academy of Sciences, Beijing 100190, China, also with the Brainnetome Center, Institute of Automation, Chinese Academy of Sciences, Beijing 100190, China, and also with the National Laboratory of Pattern Recognition, Institute of Automation, Chinese Academy of Sciences, Beijing 100190, China (e-mail: trichtu@gmail.com; hangtian@gmail.com; shiweiyang2017@ia.ac.cn; luyuheng2018@ia.ac.cn; liwen2016@ia.ac.cn; zhengyi.yang@ia.ac.cn; lingzhong.fan@ia.ac.cn).

Yu Zhang is with the Research Center for Healthcare Data Science, Zhejiang Lab, Hangzhou 311100, China (e-mail: yuzhang2bic@gmail.com).

Junjie Zhuo is with the School of Biomedical Engineering, Hainan University, Haikou 570228, Haikou China (e-mail: junjie.zhuo@hainanu.edu.cn).

Jiaojian Wang is with the School of Life Science and Technology, University of Electronic Science and Technology of China, Chengdu 610054, China (e-mail: jiaojianwang@gmail.com)

Luqi Cheng is with the School of Life and Environmental Sciences, Guilin University of Electronic Technology, Guilin 541004, China, also with the Brainnetome Center, Institute of Automation, Chinese Academy of Sciences, Beijing 100190, China (e-mail: luqi.cheng.ccm@gmail.com).

Tianzi Jiang is with the National Laboratory of Pattern Recognition, Institute of Automation, Chinese Academy of Sciences, Beijing 100190, also with the School of Artificial Intelligence, University of Chinese Academy of Sciences, Beijing 100190, China, also with the Brainnetome Center, Institute of Automation, Chinese Academy of Sciences, Beijing 100190, the School of Life Science and Technology, University of Electronic Science and Technology of China, Chengdu 610054, China, also with the CAS Center for Excellence in Brain Science and Intelligence Technology, Institute of Automation, Chinese Academy of Sciences, Beijing 100190, China, and also with the Queensland Brain Institute, University of Queensland, Brisbane, QLD 4072, Australia (e-mail: jiangtz@nlpr.ia.ac.cn).

cortical atlas that can reveal individual areal differences, which are obscured by population averaging, and can highly replicate such differences across repeated sessions[38]. The first issue to be addressed in the cerebral cartography is that the complication of individual connectivity fingerprints. It may be dynamic and influenced by different brain states [39] for a single subject, which may lower the parcellation reproducibility in practices. Second, the population characteristics of parcellations should remain on group, such as maximum probability maps (MPMs) and detected area numbers, despite of individual variability. In other words, the utilization of population priors should effectively constrain the parcellations to avoid the systematical biases in the group. Population priors should be integrated reliably into the mapping to handle the variations of the connectivity fingerprint as well as to avoid obvious outliers in the individual parcellations. Previous methods have made lots of efforts on the utilization of population priors, such as providing rough spatial locations of cortical areas or the distribution of cortical fingerprints on these locations, or iterating group connection fingerprints [13, 26, 27, 30, 37]. For example, Han et al. presented well delineation of individualized cerebral cartography by iteratively updating reference anatomical connectivities for each area, and matching them with vertex-level anatomical connectivities to identify individual cortical areas (denoted as iterative clustering (IC) methods) [26, 30], but it might present areal outliers far from its group locations when faced with fingerprint noises or population biases on certain small areas. From functional aspects, the functional connectome reflected by an individual parcellation should have more associations with related individual cognition behaviors or the illness symptoms, and provides a more precise individual measurement for the clinic practices [37, 40].

With the current situation and existing problem, machine learning methods may provide alternative solutions with their flexible modeling, powerful data fitting, and inference capabilities. First, the structure-function relationship has been widely investigated in neuroscience research for decades. A series of studies showed that each functional area has a unique anatomical connectivity fingerprint [29, 41] and that the brain activations of a functional area can be inferred from its connectivity fingerprint [28, 42]. A precise anatomical and biological ROIs (e.g., fiber tracts), rather than template-based locations for the anatomical fingerprints could reflect a reliable and explainable variations for each group area. Machine learning methods is suitable to segment an individual-level, automated ROIs. Second, brain connection fingerprints have the spatial correlation (functional or anatomical fingerprints). It implies that the spatially connectivity contexts of fingerprints within neighborhood vertexes (include itself) could hopefully provide reliable areal landmarks to be utilized in for reliable area identification rather than only itself fingerprint. The graph convolutional networks make this connectivity-context-based analysis possible on non-Euclidian geometric space (e.g., the brain cortical surface). The connectivity context of corresponding atlas areas can be extracted and learned in a machine learning framework using a few graph convolutional kernels (e.g., Chebyshev polynomials). Additionally, the trained model can inference a new data within seconds. Certain graph kernels may also be feasible on subgraphs of certain graph structure, so that the trained model can also be applied in local region with less time consumption.

With the integration of these solutions, we developed a Brain Atlas Individualization Network (BAI-Net) using group priors (in here, we use the Human Brainnetome Atlas[14] in the experiment). The presented method presented a connectivity-based (rather morphology-based) machine-learning framework for the precise location of individual functional areas with below advantages.

1) First, we used the individual-level anatomical connectivity fingerprint derived from fiber-tract embedding of the diffusion tractography to handle the connectivity complexity as well as model interpretability. The resulting individual parcellations showed a high reproducibility and biological meanings.

2) Second, the connectivity context is introduced for reliable areal identification using graph convolution networks. A vertex-level brain graph (spatial structure and fingerprints) was first constructed on cortical surface. Probabilistic weights and population locations were integrated into the loss function to search a reliable connectivity context pattens for cortical areas. The high population consistency and reliable inter-subject variations was presented, resulting an improved association between individual functional connectome and individual cognition behaviors on average.

II. Datasets and Preprocessing

HCP dataset

We used two independent datasets acquired from the Human Connectome Project (HCP) dataset, consisting of T1 weighted (T1w) data, resting-state functional MRI (rs-fMRI), as well as diffusion MRI (dMRI) data for each subject. Specifically, the BAI-Net model was trained and evaluated on the first dataset, consisting of 170 subjects (Age: 21-35) acquired from the Human Connectome Project S1200 release. The test-retest reliability of the model was then evaluated on the second dataset, consisting of 44 subjects acquired from the HCP test-retest datasets. Both datasets were analyzed using the HCP minimal preprocessing pipeline [43, 44], and the cortical surfaces of a subject were reconstructed from T1-weighted MRI data and mapped onto the standard surface template with 32k vertices per hemisphere. Diffusion MRI data had been mainly preprocessed by motion correction, eddy current distortion correction, and echo-planar images (EPI) susceptibility-induced field distortion correction. The preprocessing of the functional MRI data mainly included motion correction, EPI susceptibility-induced distortion correction, linear trend removal, and independent component analysis (ICA)-based artifact removal. Further preprocessing details can be found in the HCP preprocessing pipeline [45, 46] (https://github.com/Washington-University/HCPpipelines).

A. MASiVar dataset

An additional dataset from the Multisite, Multiscanner, and Multisubject Acquisitions for Studying Variability (MASiVar) dataset [47], consisting of 74 scans (8 scans were removed due to incomplete brain tissue data in the diffusion images) from 14

adult subjects (8 males and 6 females, age 27-47), in order to evaluate the impacts of multiple sessions, sites, and scanners. The dMRIs of these subjects were acquired from 3 cohorts using four scanners (two 3T Philips Achieva scanners used at two sites, one 3T General Electric Discovery MR750 scanner, and one 3T Siemens Skyra scanner) with at least one T1-weighted image for each subject at each session. Of the three cohorts, different scanning sequences were used in diffusion imaging, including different b-values (b = 1000 to 3000 s/mm^2) and diffusion directions (about 40~96 directions for each b value), different spatial resolutions ranging from 2.5 mm isotropic or 2.1 mm by 2.1 mm by 2.2 mm (sagittal, coronal, and axial), and so on. These diffusion images were preprocessed using the PreQual pipeline [48] with the default settings, including intensity normalization and distortion correction, as well as the Marchenko-Pastur technique[49-51]. More information on PreQual can be found at https://github.com/MASILab/PreQual.

III. Method

In this section we introduced the pipeline of Brain Atlas Individualization Network (BAI-Net), including spatial graph structure of the cortical surface, connectivity fingerprints of fiber-tract embedding, context-based node classification and its optimization.

A. Spatial graph structure of the cortical surface

Spatial graph structure of the individual brain graph was derived from the triangulated cortical surfaces (fs_LR32k surfaces) of each subject. These surfaces were extracted using the Freesurfer toolbox and Workbench commands. Each graph for each hemisphere consisted of around 30k vertices/nodes (removing the vertexes in the middle wall). The edges were constructed between each pair of two vertices that shared a triangle in the cortical surface. The brain graph was sparsely connected and highly localized in space, with each vertex only connecting with 2-6 nearest vertices on average. The brain graph architecture provided a reference structure for each vertex to search for its spatial connectivity context.

B. Connectivity fingerprints of fiber-tract embedding

Many studies showed there exists a structure-function relationship and the identification of functional area through anatomical fingerprint [28, 29, 41, 42]. In this study, the fiber-tract-based connectivity fingerprint was calculated, as the one of input in the graph convolutional network (shown in ***Fig. 1a***):

1) A surface-based probabilistic tractography algorithm was used to track 5000 streamlines throughout the whole brain, including both cortical and subcortical regions, from each vertex on the cortical surface [52-55]. The resulting streamline number had a threshold at 2 and then down-sampled to a 3 mm resolution to save computation time [56].

2) A individual-level binary mask for each of the whole-brain 72 fiber bundles was automatically segmented by a pre-trained deep-learning model TractSeg tools [57]. And the resulting mask was also down-sampled to a 3mm resolution.

3) A fiber-tract-based embedding of the probabilistic tractography was conducted from the volume space (50k+ voxels) to the fiber-tract space (72 fiber bundles). A fiber-tract element in the connectivity fingerprint was calculated by averaging the connectivity values within the fiber tract mask. All fiber-tract elements were normalized to 1 for the fingerprint of a single vertex.

Intuitively, this fingerprint means the averaged probability of anatomical fibers from a vertex to pass through each fiber tracts. Such fingerprints have biologically meaning, in the field of locating the similar functional brain areas across different non-human primate species[58].

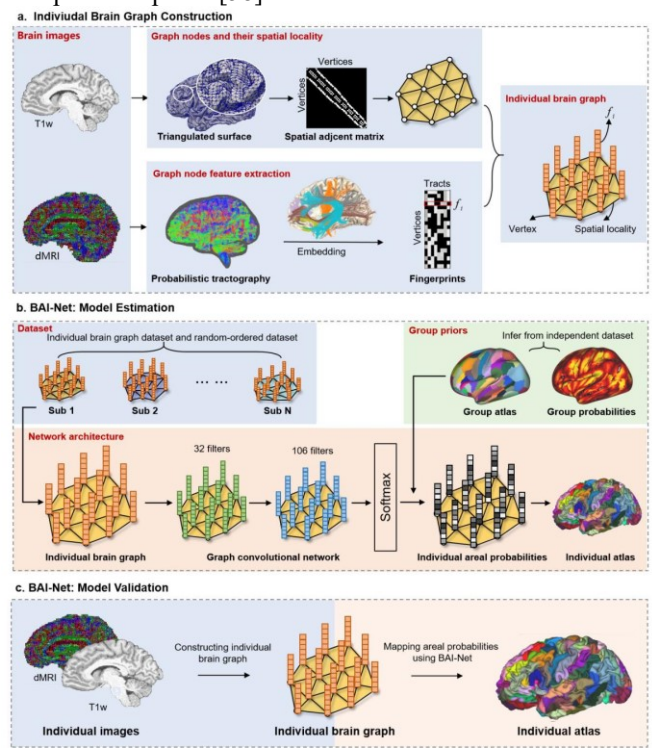

Fig. 1. Schematic diagram of the Brain Atlas Individualization Network (BAI-Net) using group priors. a: Construction of individual brain graph. b: BAI-Net: Model Estimation. c: BAI-Net: Model Validation.

C. Context-based node classification

Many previous parcellation algorithms treated each vertex or voxel independently while neglecting the context information of the neighborhoods by dividing the whole cortex into non-overlapping regions [59]. Some researchers have attempted to utilize such context information for brain parcellations. For instance, Cohen and his colleagues attempted to detect local changes in functional connectivity maps through an edge detection algorithm on the cortical surface [60]. However, only the local context from the first-order neighborhood (directly connected vertices) was considered in their method. Graph convolutional networks provide a more generalized approach for integrating the context information at each node. One type of graph convolution using Chebyshev polynomials is defined as:

$$x * g_\theta = \sum_{k=0}^{K} \theta_k T_k(L) x \qquad \text{(Eq. 1)}$$

Where $\tilde{L}$ is a normalized version of the graph Laplacian and is equal to $2L/\lambda_{max} - I$, with λ being the largest eigenvalue. θ_k is the parameter to be learned for each order of the Chebyshev polynomial T_k, ($T_k(x) = 2T_{k-1}(x) - T_{k-2}(x)$, $T_0(x) = 1, T_1(x) = x$). By using a truncated expansion of the

Chebyshev polynomial (as shown in Eq.1), the ChebNet graph convolution is naturally K-localized in the graph [61]. Specifically, when K=1, the graph convolution only considers the context information from the direct neighbors at each node. When K>1, the graph convolution also takes into account the information from a larger scale neighborhood, including nodes that can be reached within K steps of random walk on the graph. All this information is then integrated using the graph convolution. Two graph convolutional layers were stacked to enlarge the receptive fields of information integration. The GCN model took individual brain graphs as inputs, integrated the context information of brain connectivity at each vertex, and generated new representations (shown in ***Fig. 1b***).

D. Optimization of BAI-Net Method

The constructed individual brain graph dataset was used to train a GCN model with a group prior constraint (***Fig. 1b***). (In this experiment, the group prior was extracted from 210 areas on the cortical surface of the Human Brainnetome Atlas), defined based on a group of 40 healthy subjects. The group atlas was first registered from the "fsaverage" surface template to individual surface space [62]. In addition to traditional dataset, A random-ordered dataset was created by randomly assigning the connectivity fingerprints to different nodes on the graph which introduced the random state of connectivity fingerprint in a local spatial region. In this situation, the label of whole brain surface was assigned with null label. This null model was used to train the robustness of the BAI-Net model when facing abnormal inputs such as distortions in brain anatomy. There were C+1 labels in a training model (C cortical areas plus a null label per hemisphere).

A one-hot encoding was generated at each vertex to indicate the labels of the cortical areas in the group atlas. This one-hot encoding vector was then used to modify the loss function for the GCN. Specifically, the GCN model takes an individual brain graph $\mathcal{G} = (\mathcal{V}, \mathcal{E}, \mathcal{F})$ as inputs, where $\mathcal{V}$ is the set of vertices (around 30k per hemisphere) in the cortical surface, $\mathcal{E}$ is the set of edges, showing whether two vertices share a common triangle in the surface, and $\mathcal{F} \epsilon \mathbb{R}^{N \times T}$ is the set of feature vectors indicating the connectivity fingerprints f_i defined on each vertex, N is the number of vertices , T is the number of fiber tracts (here N around 30k and T =72). Using the validation dataset, optimal parameters for the two-layer graph model is chosen. The learned graph representations extracted from the last graph convolutional layer were then projected to a 106-dimensional probability vector at each vertex using the softmax function. The K-L divergence was used to calculated the difference between the group prior $y_{i,k}$ (one-hot encoding) and the predicted areal probability $p_{i,k}$ at each vertex v_i for each region k . The weight of uncertainty w_i at each vertex was inferred from the populational probability map of the group atlas. Thus, the final loss function was defined as follows:

$$Loss = \sum_{i=1}^{N} w_i \sum_{k=0}^{K} y_{i,k} \log(p_{i,k}) \qquad \text{(Eq.2)}$$

The benefits of using the above loss function include: 1) High contributions of the vertices near the center of regions help to obtain a high level of inter-subject alignment for the global topographic organization. 2) Small contributions of the vertices at the borders of regions help retain the inter-subject variability to some degree and allow the mismatching of label assignments in the local architecture.

IV. Statistical Analysis

A. Reproducibility and inter-subject variability of individual parcellations

The reproducibility of individual parcellations were evaluated by the areal overlaps (Dice coefficient) between individual parcellations from two sessions of the same subject using HCP test-retest dataset. Then for the inter-subject variability of parcellation, We first evaluation the areal overlaps between parcellations of different subjects in brain parcellation. The surface parcellation for each subject was converted into binary ROIs (C cortical areas in each hemisphere, one for each area), which were concatenated into a single vector. the Dice coefficient is calculated with the equation (2*A∩B)/(A + B) between two vectors for any areal overlaps mention in this articles.

Then we estimated the effect size of the inter-subject variability was measured by Cohen's d, which reveals the real inter-subject variations after removing the intra-subject variations. Thus, inter-subject variability (the effect size) was defined as:

$$V_{inter} = \frac{\mu_{inter} - \mu_{intra}}{\sqrt{\sigma_{inter}^2 + \sigma_{intra}^2}} \qquad \text{(Eq.3)}$$

where V_{inter} and σ_{inter} represent the mean and standard deviation of the variabilities between each pair of subjects, while V_{intra} and σ_{intra} represent the mean and standard deviation of the variabilities between different scans for the same subject.

We assumed that the individualized parcellation maps generated by the BAI-Net model would be able to retain the individual variability in brain morphology and connectivity. To test this hypothesis, we used different variability measures for brain parcellation (areal topography), brain morphology (modulated surface area), and brain connectivity (anatomical connectivity fingerprint). Modulated surface area is calculated by the averaged vertex area within a cortical region ('surface-vertex-areas' command in workbench software), reflecting the surface deformation degree from the template surface sphere. The variability in brain morphology was measured by the absolute difference in the modulated surface area of the same cortical region between two parcellations. The variability in anatomical fingerprint was calculated by the absolute difference in the mean areal fingerprint between two parcellations. Additional association analyses were performed between the inter-subject variability in parcellation and brain morphology and brain connectivity.

B. Group-registered and iterative clustering methods

Two individualized methods are compared in this study. One is group-registered method, that obtains individual parcellations based on group atlas in surface space. Group-

registered method maintains that the gyrus and sulcus of cortical areas are matched across subjects, which is also commonly used for atlas-based medical analysis in many studies. The group atlas on cortical surface is derived from mapping the group atlas in MNI space into the corresponding original templet, and then down-sampling into fsaverage LR32k surface space in which surface vertices are corresponded across subjects in terms of cortical gyrus and sulcus. For each subject, group registered method is mapping the fsaverage LR32k surface labels of group atlas into corresponding vertices of a subject's fsaverage LR32k surface.

Another is iterative clustering method, it iteratively updates global anatomical connection fingerprints, and matches them with vertex-level connection fingerprints to identify individual cortical areas. The iterative clustering method can be seen in ***Supplementary Methods***). The original method with the anatomical connectivity was applied on image volume space [30], we adjusted it on individual cortical surface space, details of the method can be seen in Supplementary Methods.

C. Consistency of individualized model with population atlas priors

We estimated the areal consistency of individual parcellations with a group atlas using areal overlaps with priors, areal detection rate, areal outlier rate, maximum probability maps (MPMs) similarity.

1) **Areal overlaps with priors:** the areal overlaps with priors is calculated by the region overlaps (Dice coefficient) of individual area regions with group-registered regions on fs_LR32k surface.

2) **Areal detection rate:** we also considered the areal sizes of the resulting subject parcellations relative to the population priors. If an area in an individual model was within 0.33x to 3x the size of the group area, this area was considered as being detected for this subject [13].

3) **Areal outlier rate:** the region of cortical area that exceed regions of its spatial neighborhood cortical areas in group atlas was defined as outliers. The percentage of these regions within the whole cortical surface are calculated.

4) **MPM similarity:** the maximum probability maps (MPM) were annotated as the area with the highest probability at each vertex. The similarity is calculated using spatial overlaps (Dice) of the MPM between the group atlas.

D. Individual cognition behavior prediction using areal functional connectivity

To determine whether individualized parcellations have improved the delineation of individual functional differences, individual cognition behaviors from the HCP dataset is predicted using different functional connectomes derived from group-registered, iterative clustering and the BAI-Net method, separately. We used a leave-one-out cross validation to demonstrate the improvement using 166 HCP subjects (4 monozygotic subjects are removed, but one of family members might be shared between training dataset and the validation subject). The areal functional connectivity for each session was calculated by the Pearson correlation between the average timeseries for two cortical areas. The areal functional connectivities in different sessions for the same subject were averaged. Prediction in each iteration consisted of three steps, similar to a previous method [25]. 1) **Feature selection**: The areal functional connectivity was calculated using the Pearson coefficient between two areal resting functional timeseries. We selected significant functional connectivity with corresponding cognition behavior under a certain p value threshold (0.1, 0.05 or 0.01). 2) **Model building**: We fitted a simple linear regression between a cognition behavior and selected functional connectivities using the training data. 3) **Model prediction**: The individual cognition behavior was predicted by a trained linear model using the testing data. For each cognition behavior, the prediction performance was evaluated by all the testing predictions and observations. For a behavior, the maximum accuracy among different level of feature selections was recorded. And for the negative accuracy of a behavior, due to its unconvinced performance, these performances are set to 0 in the averaged performance of all behaviors. The same prediction processes were conducted using functional connectomes derived from different parcellations separately

V. EXPERIMENTAL RESULTS

A. Graph model training setting

Through the validation testing, the model super-parameters were optimized through the grid research to achieve a better performance but with lower model parameters to avoid overfitting. A 5th-order graph convolution was used in GCN with 32 convolutional kernels in the first GCN layer and 106 kernels in the second GCN layer. We used Adam as the optimizer with an initial learning rate of 0.01 (decreased to 0.0001 after the 5th epoch). An additional l2 regularization of 0.0005 on weights was used to control model overfitting and noise in the imaging data. The network was trained on 100 subjects for 50 epochs with the batch size set to 1 (processing one subject at a time) using traditional dataset and random-order dataset respectively and evaluated on the validation set of 20 subjects at the end of each training epoch. The best model over 50 training epochs, that is, the one that achieved the lowest loss on the validation set, was saved and further evaluated on the independent test set of 50 subjects. During model evaluation (***Fig 1c***), an individual brain graph was first constructed from the test subject, using surface construction, diffusion tractography, and fiber-tract embedding. Then, the GCN model took the brain graph constructed from the target subject as input and predicted the areal probability vector at each vertex. Next, each vertex was assigned to the one of the 105 cortical areas for which it showed the highest probability. The predicted labels from both hemispheres were then combined to generate the final individualized brain atlas. The graph model is training with Tensorflow deep-learning framework using the GeFore GTX 1080K.

B. Test-retest reliability of individual-specific areal pattern

The reliability of these individual-specific areal pattern was evaluated using the HCP test-retest datasets, consisting data from 44 healthy subjects, who had structural, diffusion, and functional MRI data from two independent sessions and no shared subjects with the above HCP testing dataset. The intra- (between the test and retest sessions of the same subject) and

inter-subject (between different subjects from the same session) similarities of the individualized parcellation maps (as shown in ***Fig. 2a***) were evaluated by calculating the Dice score between the one-hot encodings of each brain parcel and averaging the scores within each hemisphere.

The result was that highly reproducible parcellation maps were generated at the subject level, as indicated by the consistency between the test and retest sessions (Dice = 0.901±0.020 and 0.902±0.012 for the left and right hemispheres, respectively). At the meantime, substantial inter-subject variability was observed especially at the borders between different cortical regions, as indicated by a low value (<0.5) in the probability map (***Fig. S2)***. The inter-subject variability maps followed the same topographic pattern on the test and retest sessions (*Pearson r* = 0.989). Moreover, the test-retest reliability analysis, as measured by the Dice score between the individual parcellation maps, revealed a much lower reproducibility between subjects (Dice = 0.726±0.029 and 0.726±0.033 for the left and right hemisphere) as compared to the intra-subject results (p values < 10^{-42} and <10^{-57} for the left and right hemispheres).

Examples of individualized parcellation maps in the right hemisphere and their test-retest reliability are shown in ***Fig. 2b*** (maps of the left hemisphere shown in ***Fig. S3***). The BAI-Net model detected large variations in the shapes and boundaries of the A39rv, A45c, and cLinG in the three illustrated subjects. However, their topographic organization, i.e., the spatial locations of A39rv, A45c, and cLinG as well as their relationships with the surrounding brain areas, were highly consistent between the test and retest sessions. Our results indicated that, in contrast to the registration-based group atlas, the BAI-Net parcellation scheme not only maintained the global inter-subject alignment in brain structure but also retained reliable individual characteristics of brain morphology and connectivity in the local topographic organization.

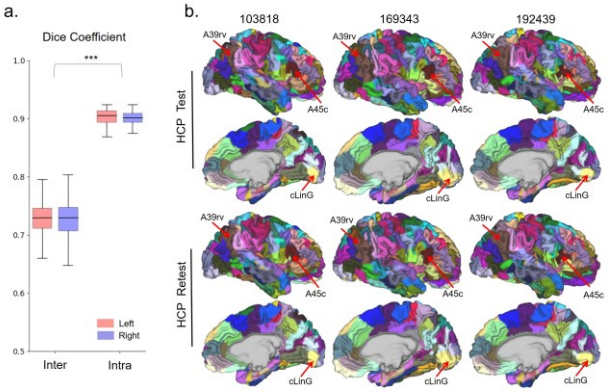

Figure 2. Reliability of the BAI-Net individualized parcellation on the HCP test-retest dataset. a: Inter- and intra-subject overlaps in individual parcellations of HCP test-retest subjects. b: Examples of individual parcellations for three randomly chosen subjects.

C. High parcellation generalizability over multiple scanners

The generalizability of the individualized parcellations derived from the BAI-Net model (pre-trained on HCP testing dataset) was further evaluated using the MASiVar dataset, which consists of 74 repeated acquisitions of 14 healthy subjects after combining 3 cohorts. The BAI-Net parcellation yielded much higher variability between different subjects than within the same subject, not only when using the same scanners (Dice score=0.860±0.024 and 0.707±0.027, respectively for intra-subject and inter-subject pairs), but also when using different scanners (Dice score=0.830±0.015 and 0.703±0.025, respectively for intra-subject and inter-subject pairs). It is worth noting that both the intra- and inter-subject similarity were slightly lower in the multi-scanner dataset (MASiVar) than those in the single-scanner HCP dataset (***Fig. 3a***). The BAI-Net model captured reliable individual-specific signatures when using data acquisitions from the same subject but different scanners (***Fig. 3b***). In addition, the model detected large variations in the brain parcellation across different subjects. Our results demonstrated that the BAI-Net model generalized well on large populations either acquired from a single scanner or using multiple scanners.

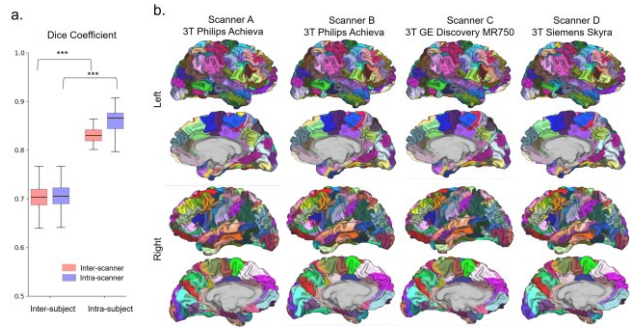

Figure 3. Generalizability of BAI-Net model on multiple scanners using the MASiVar dataset. a: The similarity of the individualized parcellation maps between the same scanner (intra-scanner) and different scanners (inter-scanner) for the same subject (intra-subject) and different subjects (intra-subject). b: Four examples of brain parcellations on the subject 'sub-cIls04' using dMRI images acquired from different scanners. The box represents the first and third quartiles in the distribution of the Dice scores.

D. Inter-subject variability in brain parcellation was associated with both brain connectome and morphology

Besides the model reproducibility, we quantified the inter-subject variability of parcellations with areal topography by the effect size (Cohen's *d*), which was computed the differences of the region overlaps (Dice scores) between inter-subject pairs and intra-subject pairs. On this basis, we further tested the associations of areal topography variability with brain morphology (modulated surface ar ea) and connectome (areal anatomical fingerprint) using the HCP test-retest dataset (***Fig. 4***).

As shown in ***Fig. 4***, the BAI-Net individualized parcellation maps showed a large effect size of inter-subject topography variability at the whole-brain level. The topographic pattern of the effect size in the BAI-Net parcellations followed the functional and connectional gradient of the cortical organization[17]. Generally speaking, relatively small inter-subject variations were observed in the primary cortex, e.g., the primary motor and sensory cortex. Higher effect sizes were detected in the association cortex, especially for brain regions that are involved in higher-order cognitive functions, e.g., the middle frontal gyrus (MFG) and inferior parietal lobule (IPL), which also exhibited greater functional variability than the other parts of the cerebral cortex[17]. Similar topographic organization was observed in the effect size maps for modulated surface area, anatomical fingerprint.

Moreover, we found a strong association in the variability maps between the brain parcellation and the connectivity fingerprints (r = 0.51, $p < 10^{-14}$). By contrast, a significant association with brain morphology was only detected for regions with relatively low variability in the brain parcellation (effect size < 2.3, r = 0.65, $p < 10^{-13}$) but not for highly variable brain regions (effect size ≥ 2.3, r = 0.17, p = .08). Our results indicated that the heterogeneity of the cortical organization revealed by the individualized parcellation maps was highly attributable to individual differences in brain connectivity rather than solely relying on variations in brain morphology.

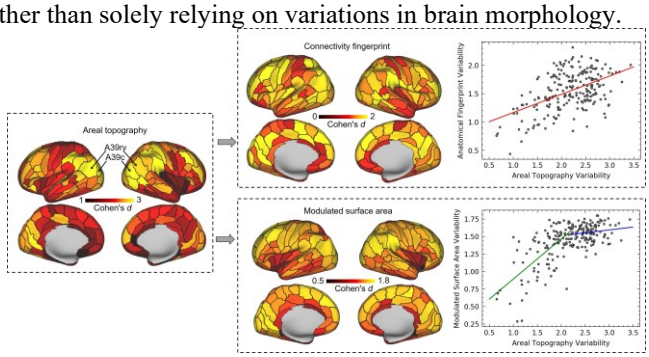

Figure 4. Inter-subject variability of individualized parcellations using the HCP test-retest dataset. Inter-subject areal variability for areal topography (left side) are estimated by the effect size (Cohen's d score), as well as for connectivity fingerprint (first column on right side) and modulated surface area (second column on right side). The regression models were fit the relationship between areal topography and the other two features. Each dot in the right plot indicated one cortical area in the parcellation map.

E. Performance comparisons among parcellations

1) Higher group consistency: areal overlaps with priors, areal detection rate, areal outliers and MPM similarity

As the reliable inter-subject parcellations revealed by individual parcellations, rather than group-registered parcellations, we first investigate the general performance on group consistency between individualized methods using HCP test-retest dataset, the mean outlier rate of BAI-Net-based individual parcellations was 1.78%±0.29% while it was 4.10%±0.34% for IC-based individual parcellations (examples in ***Fig S6***). Moreover, BAI-Net method also shown the high areal detection rate (98.7%) than IC-based method (94.5%) across HCP testing subjects. And MPM of BAI-Net-based parcellations also shown higher overlaps with group priors (88.0%) than IC-based method (82.8%) in ***Fig. 5***. These measurements indicates that BAI-Net method might has a high group-consistent and reliable individual parcellations than IC method. The BAI-Net individualized parcellation generally followed a topographic pattern that was similar to that of the group atlas (mean Dice coefficient = 0.762±0.025), in comparison of 0.703±0.049 Dice coefficient for IC-based method. Although lower areal group overlap for IC-based method might means a higher inter-subject variability, this assumption may not be supported by the inter-subject similarity of IC-based parcellations is 0.804±0.080)

In addition, in the random test (randomly assignment of the connectivity fingerprints to different nodes), 99.9% of the vertices was identified with the null label. This might be hard for IC-based method because the absence of null label makes it unable to identify high noise regions in the MRI data. Our results indicated that the BAI-Net individualized parcellation mostly retained the global topographic organization of cerebral cortex that inherited from the group atlas, and made considerable adjustment to the local alignments by aggregating the context information of connectional architecture on individual brains.

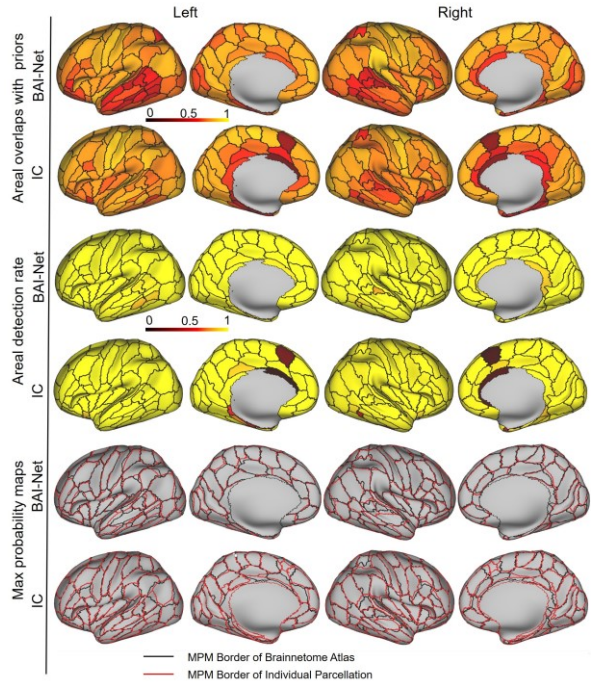

Figure 5. Group consistency of the individual parcellations using BAI-Net and IC methods using HCP test dataset, including areal overlaps with prior areal, areal detection rate, the border of MPMs from parcellations based on two methods respectively.

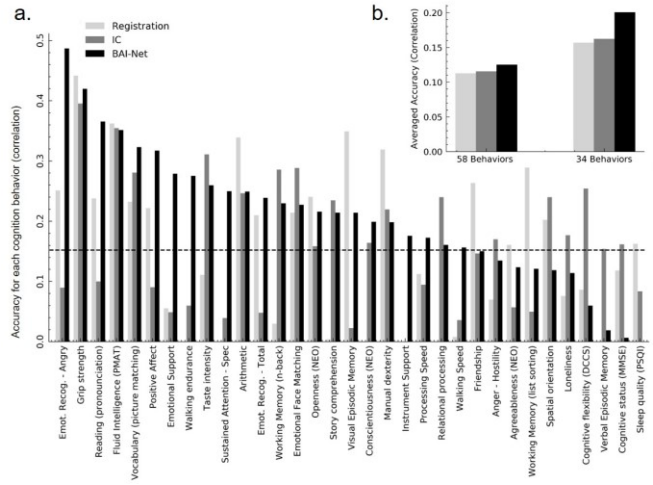

Figure 6 The prediction accuracy (correlation) using functional connectome of parcellations derived from group-registered, IC and BAI-Net methods in the leave-one-out cross validation. a. the prediction accuracy for 34 cognition behaviors significantly predicted by at least one of functional connectomes. b: there are 58 cognition behaviors, as well as 34 significantly predicted ones.

2) Improved predictions on individual cognitive scores

Better inter-subject functional alignment eventually improves brain-behavior associations, i.e., predicting behavioral scores based on brain connectivity. To test this, we applied a simple linear model to predict individual cognition behaviors using the functional connectome of parcellations derived from the group-registered, IC or BAI-Net methods,

respectively. We estimated the performance on 58 cognition behaviors (the same with [33, 37]), using Pearson correlation (r score) to quantify the association between predicted values and observed behavioral scores in the leave-one-out cross validation. Among these scores, 34 behaves are significantly predicted ($p < .05$) by at least one of functional connectomes extracted from these parcellations. We listed the mean accuracy of these behaviors from different methods. As shown in ***Fig. 6***, the mean accuracy of 58 behaviors were r = 0.112,0.115 and 0.125 for group-registered, IC and BAI-Net methods, respectively. And the mean accuracy of 34 significant predicted behaviors were r = 0.157, 0.162 and 0.201 for three methods.

3) Regional cortical parcellation for certain target location in a time-saving manner.

Another advantage of BAI-Net method, compared with iterative clustering method, is that it can be worked in a regional mode. The construction of individual brain graph does not require the whole surface and the same graph nodes across subjects. The parameters of model can be generalized into any subgraph of a global brain graph but still keep most of parcellation information from global mode. As shown in ***Fig. 7***, three subjects still keep high overlaps with global parcellations. Regional individual parcellation also means that the probabilistic tracking process (around 40 mins using GPUs per hemisphere) in the global parcellation could be proportionally reduced based on the scope of the selected region. The selected region (including around 2700 vertices, ***Fig 7a***) only using less than 4 mins in the anatomical tracking processing, which could be highly time-saving for the clinical uses, especially for the certain location, such as the left dorsolateral prefrontal cortex (dlPFC). In contrast, iterative clustering method needs updating whole surface signals and might be sensitive to the selected ROI, which could not be proper for the reginal parcellation.

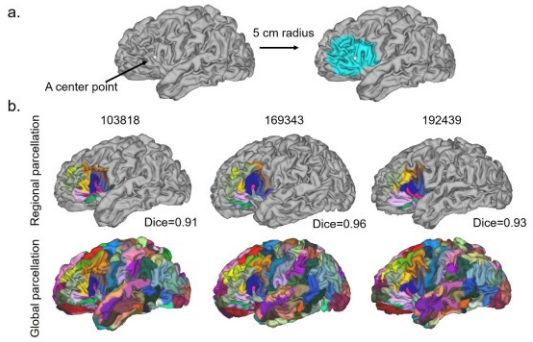

Figure 7. Regional parcellation for certain target cortical areas. a) the region selection on cortical surface within a 5cm geodesic line. b) BAI-Net parcellation comparison in regional and global mode using the same subjects (subject ID: 103818, 169343, 192439). There are high overlaps (Dice=0.91, 0.96, 0.93) with global parcellation for three subjects when using BAI-Net method.

VI. Discussion

An individualized brain atlas is one approach to understanding individual behaviors, physiology, and associated brain diseases. We developed the brain atlas individualization network (BAI-Net) from a brain-connectivity view of a cortical surface to automatically parcellate the cerebral cortex into segregated areas. The BAI-Net integrates the explainable representation of anatomical fingerprints with the connection context extracted by graph convolution networks in irregular space. The presented method provided highly reproducible, individual-specific brain atlases under a variety of acquisition environments. The resulting individual parcellations showed distinct inter-subject variability that was obscured by using anatomical registration from a group atlas. The population characteristics of individual parcellation are highly correlated with group atlas priors. The presented model was able to improve the associations of atlas-based functional connectome with many individual cognition behaviors.

Traditionally, individual parcellations were derived from registration method (e.g., sulcus-based registration on cortical surface) between individual T1w/T2w images and a standard group atlas. Such methods (no matter on the image-level CNN [63] or surface-level GCN framework [64]) used the extrinsic geometry of the cerebral cortex as the features across subjects but neglect the intrinsic connectional architecture of an individual brain. However, several studies indicated that such inter-subject areal variabilities (e.g., atypical parcellation topography) of individualized cerebral cartography have a more significant association with individual cognitions, behaviors, gender, and mental diseases than using sulcus-based surface registration [13, 26, 30, 32, 33, 40, 65]. But, the machine learning-based method have not been investigated fully in connectivity-based atlas individualization with group atlas priors due to the high-dimension and complicity of the connectivity.

Among these connectivity-based methods, functional-fingerprint-based methods are dominant and direct in the cerebral cartography, providing a lot of perspective and practical works for the clinics [13, 37, 40]. On the other side, structure covariations and anatomical fingerprints could reflect the individual functional variability to some extent [29, 42, 66], but are still less investigated and involved in the brain atlas individualization. The anatomical fingerprints have the advantages in reproducibility in many studies, compared with functional fingerprints [66]. Although high reproducibility is often companied with high individual similarity, it still useful for telling a precise location in practices, without the situation for multiple image acquisitions.

In presented BAI-Net method, fiber-tract-based connectivity fingerprints [58] have the following advantages for delineating the individual brain anatomy: 1) **Long-distance, whole-brain connectivity.** Short-distance connectivity in the probabilistic tracking is always more numerous and has a higher probability than long-distance connectivity. Placing too much attention on short connectivity (e.g., IC method), could eclipse the critical roles of long-range connectivity in identifying an area. Moreover, presented fingerprints reflect not only cortical-cortical connections but also subcortical-cortical connections. 2) **Global-range biological distinction.** Local areal features (e.g., fractional anisotropy, myelin maps) lack the ability to make such global-range distinctions[13, 67], when they are applied to a distant brain region. The fiber-tract-based fingerprint can identify all the areas together in one time each hemisphere, thus greatly reducing the number of classifiers, as well as parcellating regionally to save computation time. Such global distinction of fingerprints even exists across different higher primate species [41, 58]. 3) **Individual-level precision.**

Previous methods also used image registration from a standard template to locate the fiber tract positions in individuals [58]. The BAI-Net, which adopts a deep-learning-based tool (TractSeg), was able to locate 72 individual fiber tracts more accurately than registration methods. The fingerprints are derived with a more precise, well-defined anatomical reference basis for cross-subject analysis.

Like the connectivity fingerprints, the approaches to handling the relationships between the connectivity fingerprints and the cortical areas using group priors are also manifold: clustering, generative or discriminative methods [13, 22, 26, 30, 33, 36]. 1) **Surface-based graph analysis.** The fine-grained surface in the Human Connectome Project-style processing provides a more accurate spatial localization of the cortical areas from which it is suitable to select the neighborhood of a vertex on the cortical surface[68]. 2) **Connectivity context identification.** For the anatomical-connectivity-based method, iterative clustering method might not have a reliable consistency with group priors on surface in terms of several indicators when the number of cortical areas gets larger. The connectivity context provides a more robust representation of areal connectivity from a group atlas than iterative clustering method, shown in the detect rate, outlier rate and MPM overlaps measurements.

The time consumption of the BAI-Net method to inference the cerebral cartography of a new subject is around 3h on the Centos 6 Linux system, with a preprocessed individual cortex surface. And the model supported the regional parcellation**.** The experiment shown that parcellating in a small region still works and highly overlaps with the whole-surface parcellation. This mode could partially solve the time problem of probabilistic tracking when only regional areas are needed.

BAI-Net provides an applicable individualization framework for probabilistic group atlases with the assistance of graph neural networks. A reliable topological arrangement of the cerebral cortex in individuals provides a basis for precise individual brain cortical analysis. Obtaining such an individualized analysis can enable the localization of high-confidence physiological biomarkers, the exploration of individual structural and functional relationships, and the utilization of practical applications, such as identifying individual cortical areas for population-significant analysis, locating the target areas for transcranial magnetic stimulation (TMS) and deep brain stimulation (DBS) therapies, and reducing functional impairment in neurosurgery.

However, the presented model only used the information from structure and diffusion MRI, it might be better to achieve a better individual parcellations when multi-modality images are involved. The Glasser et al presented an example of multi-modality method. It would be better to achieve a high-reproducibility parcellation than recent performance when anatomical connectivity is involved.

VII. CONCLUSION

The presented pipeline and its methodological rationale will be also useful for individualizing other atlases (Julich-Brain[7]) based on individual anatomical connectivity profiles rather than based on morphological registration from individual T1w images. The connectivity fingerprints and connectivity context derived from graph model, provide a more reliable and highly reproducible individual parcellations. Based on the individual parcellations as well as areal inter-subject variations, the functional connectomes could achieve a better association with many individual cognition behaviors on average than group-registered and iterative clustering methods.

REFERENCES

[1].Brodmann., K., *Vergleichende Lokalisationslehre der Großhirnrinde in ihren Prinzipien dargestellt auf Grund des Zellenbaues*. leipzig Germany: von Johann Ambrosius Barth, 1909.

[2].Vogt., C. and O. Vogt., *Allgemeinere Ergebnisse unserer Hirnforschung*. Journal für Psychologie und Neurologie, 1919. **25**(Suppl. 1): p. 273-462.

[3].Collins, D.L., P. Neelin, T.M. Peters and A.C. Evans, *Automatic 3D intersubject registration of MR volumetric data in standardized Talairach space.* J Comput Assist Tomogr, 1994. **18**(2): p. 192-205.

[4].Zilles, K. and K. Amunts, *Centenary of Brodmann\"s map — conception and fate.* Nature Reviews Neuroscience, 2010. **11**(2): p. 139-145.

[5].Hawrylycz, M.J., et al., *An anatomically comprehensive atlas of the adult human brain transcriptome.* Nature, 2012. **489**(7416): p. 391-399.

[6].K. Amunts, et al., *BigBrain: An Ultrahigh-Resolution 3D Human Brain Model.* Science, 2013. **340**(6139): p. 1472-1475.

[7].Amunts, K., H. Mohlberg, S. Bludau and K. Zilles, *Julich-Brain: A 3D probabilistic atlas of the human brain's cytoarchitecture.* Science, 2020.

[8].Yeo, B.T., et al., *The organization of the human cerebral cortex estimated by intrinsic functional connectivity.* J Neurophysiol, 2011. **106**(3): p. 1125-65.

[9].Power, J.D., et al., *Functional Network Organization of the Human Brain.* Neuron, 2011. **72**(4): p. 665-678.

[10].Van Essen, D.C., *Cartography and Connectomes.* Neuron, 2013. **80**(3): p. 775-790.

[11].Shen, X., F. Tokoglu, X. Papademetris and R.T. Constable, *Groupwise whole-brain parcellation from resting-state fMRI data for network node identification.* Neuroimage, 2013. **82**: p. 403-415.

[12].Gordon, E.M., T.O. Laumann, B. Adeyemo, J.F. Huckins and S.E. Petersen, *Generation and Evaluation of a Cortical Area Parcellation from Resting-State Correlations.* Cerebral Cortex, 2014. **26**(1): p. 288-303.

[13].Glasser, M.F., et al., *A multi-modal parcellation of human cerebral cortex.* Nature, 2016. **536**(7615): p. 171-+.

[14].Fan, L., et al., *The Human Brainnetome Atlas: A New Brain Atlas Based on Connectional Architecture.* Cereb Cortex, 2016. **26**(8): p. 3508-26.

[15].Zuo, X.N. and X.X. Xing, *Test-retest reliabilities of resting-state FMRI measurements in human brain functional connectomics: A systems neuroscience perspective.* Neuroscience and Biobehavioral Reviews, 2014. **45**: p. 100-118.

[16].Toga, A.W., P.M. Thompson, S. Mori, K. Amunts and K. Zilles, *Towards multimodal atlases of the human brain.* Nature Reviews Neuroscience, 2006. **7**(12): p. 952-966.

[17].Mueller, S., et al., *Individual variability in functional connectivity architecture of the human brain.* Neuron, 2013. **77**(3): p. 586-95.

[18].Fox, M.D., H.S. Liu and A. Pascual-Leone, *Identification of reproducible individualized targets for treatment of depression with TMS based on intrinsic connectivity.* Neuroimage, 2013. **66**: p. 151-160.

[19].Fox, M.D., et al., *Resting-state networks link invasive and noninvasive brain stimulation across diverse psychiatric and neurological diseases.* Proceedings of the National Academy of Sciences of the United States of America, 2014. **111**(41): p. E4367-E4375.

[20].Dickie, E.W., et al., *Personalized Intrinsic Network Topography Mapping and Functional Connectivity Deficits in Autism*

Spectrum Disorder. Biological Psychiatry, 2018. **84**(4): p. 278-286.
[21].Patriat, R., et al., *Individualized tractography-based parcellation of the globus pallidus pars interna using 7T MRI in movement disorder patients prior to DBS surgery.* 2018. **178**: p. 198-209.
[22].Gordon, E.M., et al., *Precision Functional Mapping of Individual Human Brains.* Neuron, 2017. **95**(4): p. 791-807 e7.
[23].Fisher, A.J., J.D. Medaglia and B.F. Jeronimus, *Lack of group-to-individual generalizabilityis a threat to human subjects research.* Proceedings of the National Academy of Sciences of the United States of America, 2018. **115**(27): p. E6106-E6115.
[24].Fan, L., *Mapping the Human Brain: What is the Next Frontier?* The Innovation, 2020. **2**(1): p. 100073.
[25].Finn, E.S., et al., *Functional connectome fingerprinting: identifying individuals using patterns of brain connectivity.* Nature Neuroscience, 2015. **18**(11): p. 1664-1671.
[26].Wang, D.H., et al., *Parcellating cortical functional networks in individuals.* Nature Neuroscience, 2015. **18**(12): p. 1853-1860.
[27].Gordon, E.M., et al., *Generation and Evaluation of a Cortical Area Parcellation from Resting-State Correlations.* Cereb Cortex, 2016. **26**(1): p. 288-303.
[28].Osher, D.E., et al., *Structural Connectivity Fingerprints Predict Cortical Selectivity for Multiple Visual Categories across Cortex.* Cerebral Cortex, 2016. **26**(4): p. 1668-1683.
[29].Passingham, R.E., K.E. Stephan and R. Kotter, *The anatomical basis of functional localization in the cortex.* Nat Rev Neurosci, 2002. **3**(8): p. 606-16.
[30].Han, M., et al., *Individualized Cortical Parcellation Based on Diffusion MRI Tractography.* Cereb Cortex, 2019.
[31].Schaefer, A., et al., *Local-Global Parcellation of the Human Cerebral Cortex from Intrinsic Functional Connectivity MRI.* Cerebral Cortex, 2018. **28**(9): p. 3095-3114.
[32].Salehi, M., A. Karbasi, X. Shen, D. Scheinost and R.T. Constable, *An exemplar-based approach to individualized parcellation reveals the need for sex specific functional networks.* Neuroimage, 2018. **170**: p. 54-67.
[33].Kong, R., et al., *Spatial Topography of Individual-Specific Cortical Networks Predicts Human Cognition, Personality, and Emotion.* Cereb Cortex, 2019. **29**(6): p. 2533-2551.
[34].Li, M., et al., *Performing group-level functional image analyses based on homologous functional regions mapped in individuals.* PLoS Biol, 2019. **17**(3): p. e2007032.
[35].Gordon, E.M., et al., *Individual-specific features of brain systems identified with resting state functional correlations.* Neuroimage, 2017. **146**: p. 918-939.
[36].Chong, M., et al., *Individual parcellation of resting fMRI with a group functional connectivity prior.* Neuroimage, 2017. **156**: p. 87-100.
[37].Kong, R., et al., *Individual-Specific Areal-Level Parcellations Improve Functional Connectivity Prediction of Behavior.* Cerebral Cortex, 2021. **00**: p. 1-24.
[38].Zuo, X.N., T. Xu and M.P. Milham, *Harnessing reliability for neuroscience research.* Nature Human Behaviour, 2019. **3**(8): p. 768-771.
[39].Salehi, M., et al., *There is no single functional atlas even for a single individual: Functional parcel definitions change with task.* Neuroimage, 2019: p. 116366.
[40].Wang, D.H., et al., *Individual-specific functional connectivity markers track dimensional and categorical features of psychotic illness.* Mol Psychiatry, 2018.
[41].Mars, R.B., et al., *Comparing brains by matching connectivity profiles.* Neurosci Biobehav Rev, 2016. **60**: p. 90-7.
[42].Wu, D., et al., *Hierarchy of Connectivity-Function Relationship of the Human Cortex Revealed through Predicting Activity across Functional Domains.* Cereb Cortex, 2020.
[43].Van Essen, D.C., et al., *The WU-Minn Human Connectome Project: An overview.* Neuroimage, 2013. **80**: p. 62-79.
[44].Glasser, M.F., et al., *The minimal preprocessing pipelines for the Human Connectome Project.* Neuroimage, 2013. **80**: p. 105-24.
[45].Smith, S.M., et al., *Advances in functional and structural MR image analysis and implementation as FSL.* Neuroimage, 2004. **23**: p. S208-S219.
[46].Jenkinson, M., C.F. Beckmann, T.E. Behrens, M.W. Woolrich and S.M. Smith, *Fsl.* Neuroimage, 2012. **62**(2): p. 782-790.
[47].Cai, L.Y., et al., *MASiVar: Multisite, Multiscanner, and Multisubject Acquisitions for Studying Variability in Diffusion Weighted Magnetic Resonance Imaging.* bioRxiv, 2020: p. 2020.12.03.408567.
[48].Cai, L.Y., et al., *PreQual: An automated pipeline for integrated preprocessing and quality assurance of diffusion weighted MRI images.* Magnetic Resonance in Medicine, 2021.
[49].Veraart, J., et al., *Denoising of diffusion MRI using random matrix theory.* Neuroimage, 2016. **142**: p. 384-396.
[50].Veraart, J., E. Fieremans and D.S. Novikov, *Diffusion MRI Noise Mapping Using Random Matrix Theory.* Magnetic Resonance in Medicine, 2016. **76**(5): p. 1582-1593.
[51].Cordero-Grande, L., D. Christiaens, J. Hutter, A.N. Price and J.V. Hajnal, *Complex diffusion-weighted image estimation via matrix recovery under general noise models.* Neuroimage, 2019. **200**: p. 391-404.
[52].Behrens, T.E.J., H.J. Berg, S. Jbabdi, M.F.S. Rushworth and M.W. Woolrich, *Probabilistic diffusion tractography with multiple fibre orientations: What can we gain?* Neuroimage, 2007. **34**(1): p. 144-155.
[53].Jbabdi, S., S.N. Sotiropoulos, A.M. Savio, M. Grana and T.E.J. Behrens, *Model-based analysis of multishell diffusion MR data for tractography: How to get over fitting problems.* Magnetic Resonance in Medicine, 2012. **68**(6): p. 1846-1855.
[54].Hernandez, M., et al., *Accelerating Fibre Orientation Estimation from Diffusion Weighted Magnetic Resonance Imaging Using GPUs.* Plos One, 2013. **8**(4).
[55].Hernandez-Fernandez, M., et al., *Using GPUs to accelerate computational diffusion MRI: From microstructure estimation to tractography and connectomes.* Neuroimage, 2019. **188**: p. 598-615.
[56].Li, H., et al., *ATPP: A Pipeline for Automatic Tractography-Based Brain Parcellation.* Frontiers in Neuroinformatics, 2017. **11**.
[57].Wasserthal, J., P. Neher and K.H. Maier-Hein, *TractSeg - Fast and accurate white matter tract segmentation.* NeuroImage, 2018. **183**: p. 239-253.
[58].Mars, R.B., et al., *Whole brain comparative anatomy using connectivity blueprints.* Elife, 2018. **7**.
[59].Eickhoff, S.B., B.T.T. Yeo and S. Genon, *Imaging-based parcellations of the human brain.* Nat Rev Neurosci, 2018. **19**(11): p. 672-686.
[60].Cohen, A.L., et al., *Defining functional areas in individual human brains using resting functional connectivity MRI.* Neuroimage, 2008. **41**(1): p. 45-57.
[61].Defferrard, M., X. Bresson and P. Vandergheynst, *Convolutional Neural Networks on Graphs with Fast Localized Spectral Filtering.* Advances in Neural Information Processing Systems 29 (Nips 2016), 2016. **29**.
[62].Fischl, B., M.I. Sereno, R.B.H. Tootell and A.M. Dale, *High-resolution intersubject averaging and a coordinate system for the cortical surface.* Human Brain Mapping, 1999. **8**(4): p. 272-284.
[63].Iqbal, A., R. Khan and T. Karayannis, *Developing a brain atlas through deep learning.* Nature Machine Intelligence, 2019. **1**(6): p. 277-287.
[64].Gopinath, K., C. Desrosiers and H. Lombaert, *Graph Convolutions on Spectral Embeddings for Cortical Surface Parcellation.* Medical Image Analysis, 2019. **54**: p. 297-305.
[65].Greene, D.J., et al., *Integrative and Network-Specific Connectivity of the Basal Ganglia and Thalamus Defined in Individuals.* Neuron, 2020. **105**(4): p. 742-+.
[66].Seidlitz, J., et al., *Morphometric Similarity Networks Detect Microscale Cortical Organization and Predict Inter-Individual Cognitive Variation.* Neuron, 2018. **97**(1): p. 231-+.
[67].Ganepola, T., et al., *Using diffusion MRI to discriminate areas of cortical grey matter.* Neuroimage, 2018. **182**: p. 456-468.
[68].Coalson, T.S., D.C. Van Essen and M.F. Glasser, *The impact of traditional neuroimaging methods on the spatial localization of cortical areas.* Proc Natl Acad Sci, 2018. **115**(27): p. E6356-E6365.